Chemical Science

RSC Publishing

EDGE ARTICLE

View Article Online
View Journal | View Issue

# Chloride, carboxylate and carbonate transport by *ortho*-phenylenediamine-based bisureas†‡

Cite this: *Chem. Sci.*, 2013, 4, 103

Stephen J. Moore,[a] Cally J. E. Haynes,[a] Jorge González,[ab] Jennifer L. Sutton,[a] Simon J. Brooks,[a] Mark E. Light,[a] Julie Herniman,[a] G. John Langley,[a] Vanessa Soto-Cerrato,[c] Ricardo Pérez-Tomás,[c] Igor Marques,[d] Paulo J. Costa,[d] Vítor Félix[d] and Philip A. Gale*[a]

Received 14th August 2012
Accepted 29th August 2012

DOI: 10.1039/c2sc21112b

www.rsc.org/chemicalscience



Highly potent but structurally simple transmembrane anion transporters are reported that function at receptor to lipid ratios as low as 1 : 1 000 000. The compounds, based on the simple *ortho* phenylenediamine based bisurea scaffold, have been studied for their ability to facilitate chloride/nitrate and chloride/bicarbonate antiport, and HCl symport processes using a combination of ion selective electrode and fluorescence techniques. In addition, the transmembrane transport of dicarboxylate anions (maleate and fumarate) by the compounds was examined. Molecular dynamics simulations showed that these compounds permeate the membrane more easily than other promising receptors corroborating the experimental efflux data. Moreover, cell based assays revealed that the majority of the compounds showed cytotoxicity in cancer cells, which may be linked to their ability to function as ion transporters.

## Introduction

The regulation of cellular ion concentration by complex membrane spanning proteins is critical for a range of biological processes.[1] Misregulation of chloride transport has been associated with myotonia, nephrolithiasis (kidney stones), Bartter's syndrome and cystic fibrosis.[2] Similarly, bicarbonate transport misregulation is linked to a range of disease states,[3] and has been linked with pathogenic mucus production in cystic fibrosis.[4] By synthesising molecules that can facilitate the transmembrane transport of chloride and bicarbonate it may be possible to develop new treatments for this type of disease. Furthermore, compounds that can facilitate $H^+/Cl^-$ symport or $Cl^-/HCO_3^-$ antiport processes may function as anticancer agents since the deacidification of acidic organelles leads to cytoplasmic acidification, an early event in apoptosis.[5] Indeed, there are a number of anticancer agents that have been reported to modulate intracellular pH. The prodiginines are one example, with the anticancer activity of these molecules linked to their ability to facilitate both $H^+/Cl^-$ symport and $Cl^-/HCO_3^-$ antiport processes.[6]

The synthesis of small molecules that function as membrane resident, mobile carriers for anions is an expanding field of research. By incorporating hydrogen-bond donor groups into a suitably lipophilic scaffold it is possible to transport anions through the hydrophobic interior of a lipid bilayer. Recent examples of such scaffolds include the steroid-based cholapods,[7] calix[4]pyrrole and its fluorinated or triazole-strapped analogues,[8] amphiphilic catechols and monoacylglycerols,[9] preorganised isophthalamides and squaramides,[10] and tripodal tris(aminoethyl)amine (tren) thioureas.[11]

Interest in this area has grown to encompass transporters (carriers or otherwise) that show activity in biological systems.[6,12] To improve the likelihood of new transmembrane transporter motifs exhibiting biological activity it is important to design compounds that have suitable absorption, distribution, metabolism, excretion and toxicity (ADMET) characteristics.[13] There are guidelines, such as Lipinski's rule of five, that

[a]*Chemistry, University of Southampton, Southampton, SO17 1BJ, UK. E mail: philip.gale@soton.ac.uk; Tel: +44 (0)23 8059 3332*

[b]*Molecular Science Institute (ICMol), Inorganic Chemistry Department, University of Valencia, Edificio de Institutos de Paterna, Apartado de Correos 22085, 46071, Valencia, Spain*

[c]*Department of Pathology and Experimental Therapeutics, Cancer Cell Biology Research Group, University of Barcelona, Barcelona, Spain*

[d]*Departamento de Química, CICECO and Secção Autónoma de Ciências da Saúde, Universidade de Aveiro, 3810 193 Aveiro, Portugal. E mail: vitor.felix@ua.pt*

† Electronic supplementary information (ESI) available: Synthetic experimental details, stability constant determinations. Membrane transport experimental and further details of the modelling work in the paper. CCDC 892348. For ESI and crystallographic data in CIF or other electronic format see DOI: 10.1039/c2sc21112b

‡ Crystal data for carbonate complex of **7**: $C_{57}H_{72}N_{14}O_{15}$, $M = 1193.29$, triclinic, $a = 14.146(2)$ Å, $b = 14.338(2)$ Å, $c = 16.719(3)$ Å, $\alpha = 86.271(8)^\circ$, $\beta = 81.687(8)^\circ$, $\gamma = 61.358(5)^\circ$, $V = 2944.5(8)$ Å$^3$, $T = 100(2)$ K, $P$ 1, $Z = 2$, 33949 reflections measured, 13317 unique ($R_{int} = 0.0279$), $R_1 = 0.0618$ [$F^2 > 2\sigma(F^2)$], $R_1 = 0.0780$ (all data). The counterions balancing the two negative charges of the carbonate ion comprise one whole and two half TEA molecules. The two half molecules lie on inversion centres and were refined using thermal parameter and geometrical restraints.

specify ranges of 'ideal' molecular properties such as molecular weight, partition coefficient and the number of hydrogen bond donors and acceptors.[14] By considering these guidelines we generated transporters that exhibit biological activity *in vivo*, such as fluorinated molecules based on indolylurea/thiourea[15] scaffolds that show promise as anticancer agents. By synthesising transporters that obey the rules of thumb defined by Lipinski and others, the possibility that these compounds will be biologically compatible is greater, *i.e.* have acceptable absorption, distribution, metabolism and excretion properties.

We have previously shown that bisurea receptors in which the two urea groups are linked by alkyl chains can promote chloride transport across phospholipid bilayers.[16] In other work we have shown that *ortho*-phenylenediamine-based bisureas are effective anion receptors.[17] We decided to explore the anion transport properties of *ortho*-phenylenediamine-based bisureas as promising candidates for biologically active ion transporters that may conform to the rules of thumb defined by Lipinski and others.[14]

Molecules developed from this scaffold have found extensive use in the field of anion complexation; we have previously reported that *ortho*-phenylenediamine-based bisureas function as selective carboxylate complexation agents,[17] whilst the analogous 4,5-dimethyl-1,2-phenylenediamine scaffold has been used to construct colorimetric anion sensors.[18] These motifs can be extended with additional hydrogen bond donor groups to yield receptors with enhanced anion affinity.[19] Trisureas and tetraureas developed in this way show good selectivity for phosphate and sulfate,[20] whilst a tripodal tren-based hexylurea functions as a sulfate extractant.[21] Extended amidourea macrocycles based on these scaffolds exhibit good selectivity towards carboxylates.[22] Replacement of the phenylene core with anthraquinone yields colorimetric sensors for the detection of $Hg^{2+}$ and $H_2PO_4^-$,[23] whilst replacement with a cyclohexyl core has been used for the chiral recognition of phosphate ions[24] and the colorimetric sensing of cyanide.[25] Further, these molecules have found other applications in crystal engineering,[26] as gelators,[27] and in catalysis.[28]

In this paper we report the transmembrane transport properties of *ortho*-phenylenediamine-based bisureas **1–8**, and compare them to monoureas **9–11**; the latter being analogues of the three most active bisurea transporters. The anion binding properties of this series of compounds were determined using $^1$H NMR titration techniques in DMSO-$d_6$/0.5% $H_2O$ mixtures. Anion transport was studied using a combination of ion selective electrode assays and fluorescence techniques in phospholipid vesicles. *In vitro* viability and fluorescence assays have been performed in order to evaluate the anticancer properties of these compounds. We show that this hydrogen bonding array is a highly potent anion transport motif with the most active compound studied showing transport at 1 : 1 000 000 receptor : lipid ratios. Effective transport at very low concentrations is a desirable feature allowing the potential use of these compounds in biological systems at low dose. Finally, *in silico* studies were also performed to bring further insights into the interactions of **5** and **6** with a lipid bilayer model.

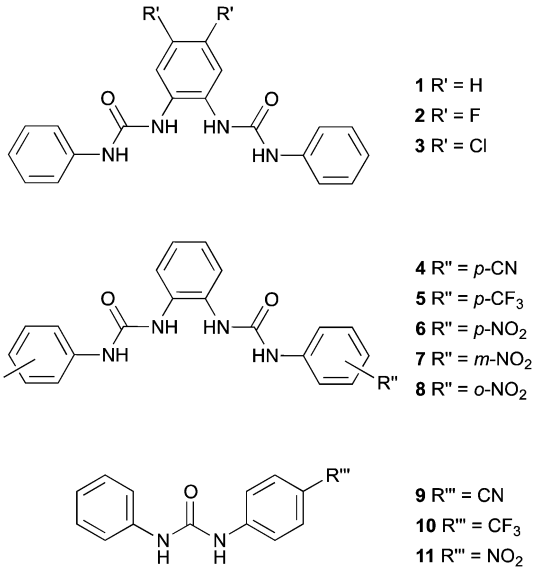


## Results and discussion

### Synthesis

We have previously reported the synthesis of compounds **1**,[17a] **3**,[17b] **6**,[17b] and **8**.[17b] Reaction of the appropriate isocyanate with *ortho*-phenylenediamine in dichloromethane/pyridine gave compounds **4**, **5** and **7** in 39%, 84% and 82% yields respectively. Compound **2** was prepared by a similar method, using 4,5-difluoro-2-nitroaniline as the starting material. Hydrogenation using Pd/C in methanol, followed by reaction with phenylisocyanate in dichloromethane/pyridine yielded compound **2** in 37% yield.

The syntheses of monoureas **9**,[29] **10**,[30] and **11** (ref. 31) have been previously reported.[32] In all cases aniline was added to the corresponding isocyanate in dichloromethane/pyridine to produce compounds **9**, **10**, and **11** in 56%, 58% and 75% yields respectively. These compounds are analogues of the three most active bisurea transporters **4**, **5** and **6**.

### Anion binding in solution

The ability of compounds **1–11** to bind anions in solution was investigated using $^1$H NMR titration techniques in DMSO-$d_6$/0.5% water (with the anions added as tetrabutylammonium (TBA) or tetraethylammonium (TEA) salts) both to provide comparability with earlier studies[33] and for solubility reasons. The binding studies were performed for anions relevant to both our transmembrane transport assays and biological systems. Where possible the change in chemical shift of the most downfield NH signal was fitted to a 1 : 1 binding model using WinEQNMR2 software.[34] The results are summarised in Table 1. Previously reported stability constants are included for comparison.[17] Fitted curves and selected Job plots can be found in the ESI.†

In general, compounds **1–11** exhibit strong 1 : 1 binding with tetraethylammonium bicarbonate, moderate 1 : 1 binding with tetrabutylammonium chloride and no significant interaction with tetrabutylammonium nitrate under the conditions of the

 

**Table 1** Stability constants $K_a$ ($M^{-1}$) for compounds **1** **11** with chloride and nitrate (added as tetrabutylammonium salts) and bicarbonate (added as tetrae thylammonium salt) in DMSO $d_6$/0.5% water at 298 K[a]

| | Chloride | Bicarbonate | Nitrate |
|---|---|---|---|
| **1** (ref. 17*a*) | 43 | 1370 | [b] |
| **2** | 73 | [c,d] | [b] |
| **3** (ref. 17*b*) | 67 | 2570[d] | [b] |
| **4** | 74 | [e] | [b] |
| **5** | 78 | 2090[d] | [b] |
| **6** (ref. 17*b*) | 78 | 3770[d,f] | [b] |
| **7** | 81 | 3140[d,f] | [b] |
| **8** (ref. 17*b*) | <10 | 826[e] | [b] |
| **9** | 41 | 2580 | [b] |
| **10** | 61 | 1380 | [b] |
| **11** | 57 | 1630[d,f] | [b] |

[a] All errors <15%. Data fitted to a 1 : 1 binding model. Binding constant obtained by following the most downfield urea NH unless stated otherwise. [b] No significant interaction observed. [c] Sigmoidal curve could not be fitted to a suitable binding model. [d] Significant broadening of urea NHs observed. [e] Reliable binding constant could not be obtained due to significant broadening of urea NHs and significant overlap of aromatic CHs. [f] Dramatic colour change observed upon addition of bicarbonate.

NMR experiments. A sigmoidal binding curve was obtained for compound **2** with tetraethylammonium bicarbonate that could not be fitted to a binding model.[35] Job plot analysis suggested 1 : 1 binding, however the plot was an unusual shape, that may be due to more complex solution phase behaviour such as deprotonation of the bound oxoanion.[33b] Significant urea NH peak broadening was observed upon addition of tetraethylammonium bicarbonate to compounds **2**, **3**, **4**, **5**, **6**, **7**, **8** and **11**. A stability constant could not be determined for compound **4** with tetraethylammonium bicarbonate due to this broadening effect, however Job plot analysis confirmed 1 : 1 binding.

Comparing functionalised receptors **2–7** with receptor **1**, it can be observed that addition of electron withdrawing substituents to either the central core or the peripheral phenyl groups increases anion affinity. In addition, it has been suggested that halogenation of the phenylene core (**2** and **3**) can aid receptor preorganisation by increasing the acidity of the phenylene CH groups, strengthening intramolecular hydrogen bonding interactions.[17b] For compounds **2–7** the binding constants obtained with tetrabutylammonium chloride are of similar magnitude whilst no significant interaction was previously reported between compound **8** and tetrabutylammonium chloride.[17b] This lack of interaction was attributed to intramolecular hydrogen bonding. The *ortho*-nitro groups may also provide a steric constraint on the binding site. Similarly, compound **8** has a significantly lower binding constant with tetraethylammonium bicarbonate than compounds **6** and **7**.

Colour changes were observed upon addition of tetraethylammonium bicarbonate to nitro-functionalised compounds **6**, **7**, **8** and **11**. Such behaviour has been reported previously in the presence of basic anions and has been attributed to deprotonation in analogous systems.[17b,18,25,36]

Interestingly, the two least active ion transporters (**1** and **8**) display the lowest affinity for both chloride and bicarbonate. The most active transporter **6** has the highest affinity of the series for bicarbonate. In addition, the monourea compounds **9**, **10** and **11** show reduced anion affinity compared to their bisurea analogues, demonstrating the impact of incorporating additional convergent hydrogen bond donor groups into the receptor scaffold.

To complement the transport studies, we attempted to titrate compounds **4**, **5** and **6** with tetrabutylammonium maleate and tetrabutylammonium fumarate in DMSO-$d_6$/0.5% $H_2O$.[37] Addition of the tetrabutylammonium dicarboxylate to the receptor solution resulted in the formation of a precipitate in both instances, preventing determination of a binding constant. Instead ESI mass spectrometry was used to examine the interaction between bisureas and dicarboxylate anions. Compound **5** was studied owing to both its good solubility and high transport activity. Negative ESI experiments with solutions of **5** and either maleic or fumaric acid revealed the formation of 1 : 1 bisurea–carboxylate complexes in the gas phase. Further, by analysing samples containing different ratios of bisurea host and carboxylate anion it was possible to determine that compound **5** binds maleate more strongly than fumarate.[38,39]

## Solid state

The solid-state behaviour of compound **7** was examined using single-crystal X-ray diffraction (Fig. 1). Tables of hydrogen bonds, data collection and refinement details, and thermal ellipsoid plots can be found in the ESI.†

Crystals were obtained by slow evaporation of a methanol–water solution of compound **7** in the presence of tetraethylammonium bicarbonate. Analysis revealed that the *meta*-nitro functionalised bisurea forms a 2 : 1 (receptor : anion) complex with carbonate, the encapsulated carbonate anion bound by eleven hydrogen-bonding interactions. All the available urea NH groups were found to be involved in hydrogen bonding the carbonate (N–O distances 2.726(2)–3.368(2) Å, N–H···O angles 139.0–166.9°). It appears that in the solid state the *meta*-nitro group does not hinder guest inclusion.

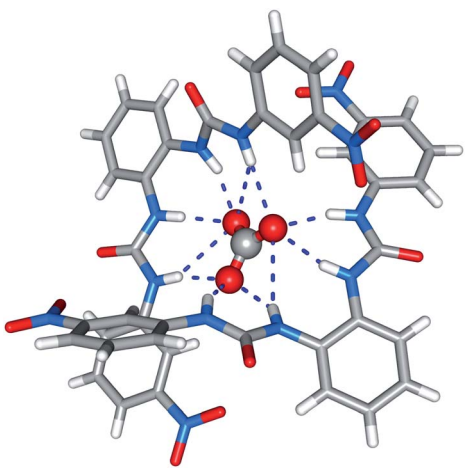

**Fig. 1** X ray crystal structure of **7** (tetraethylammonium carbonate complex). Counterions are omitted for clarity.

### Transport studies

We assessed the ability of compounds **1–11** to transport anions across phospholipid bilayers using a combination of ion selective electrode and fluorescence techniques. In a typical assay unilamellar, 1-palmitoyl-2-oleoylphosphatidyl-choline (POPC) vesicles (200 nm diameter) were prepared containing sodium chloride (488 mM with 5 mM phosphate buffer at pH 7.2) and suspended in a solution of sodium nitrate (488 mM with 5 mM phosphate buffer at pH 7.2).[40] Compounds **1–11** were added as solutions in DMSO and the resulting chloride efflux from vesicles monitored using a chloride selective electrode (Accumet). At the end of the experiment detergent (octaethylene glycol monododecyl ether) was added to lyse the vesicles. The final reading was used to calibrate the electrode to 100% chloride release.

In these assays ion transport occurs by a passive process. To maintain charge balance, ion transport must occur by either a symport or an antiport mechanism.[40] The chloride efflux in Fig. 2 could therefore be a consequence of chloride/nitrate antiport, chloride/sodium symport or HCl symport processes.

To examine the possibility of sodium/chloride co-transport, an ISE assay was performed using vesicles containing caesium chloride buffered to pH 7.2 with 5 mM phosphate buffer. The vesicles were suspended in a solution of sodium nitrate buffered to pH 7.2 with 5 mM phosphate buffer. In the event of metal chloride co-transport we would expect the rate of chloride release to be dependent on the nature of the metal cation.[8,41] The rates of chloride release for vesicles containing sodium chloride were within error of those observed for vesicles containing caesium chloride, implying that metal/chloride symport is not facilitated by these compounds (see ESI† for comparative plots).

Chloride/bicarbonate antiport is a biologically significant process.[3,6e,42] Compounds **1–11** were tested for ability to facilitate chloride exchange using a chloride selective electrode assay with vesicles containing sodium chloride (451 mM with 20 mM phosphate buffer at pH 7.2) suspended in a solution of sodium sulphate (150 mM with 20 mM phosphate buffer at pH 7.2). Compounds **1–11** were added as solutions in DMSO. After two minutes a sodium bicarbonate 'pulse' was added such that the external concentration of bicarbonate was 40 mM.

The external sulfate is more challenging to transport through a lipid bilayer than bicarbonate, due to its higher hydrophilicity.[43]

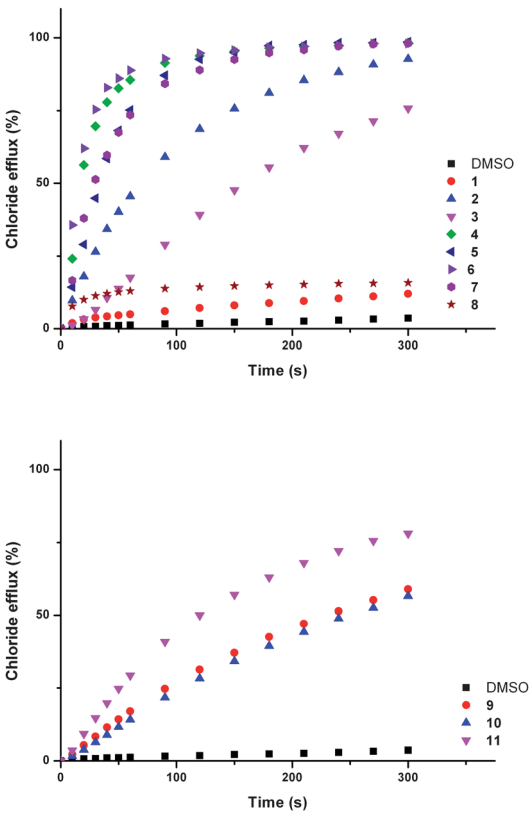


**Fig. 2** Chloride efflux promoted by a DMSO solution of compounds **1 11** (2 mol % carrier to lipid) from unilamellar POPC vesicles loaded with 488 mM NaCl buffered to pH 7.2 with 5 mM sodium phosphate salts. The vesicles were dispersed in 488 mM $NaNO_3$ buffered to pH 7.2 with 5 mM sodium phosphate salts. At the end of the experiment detergent was added to lyse the vesicles and calibrate the ISE to 100% chloride efflux. Each point represents an average of three trials. DMSO was used as a control. See Fig. S44 and S45† for versions of this figure with error bars.

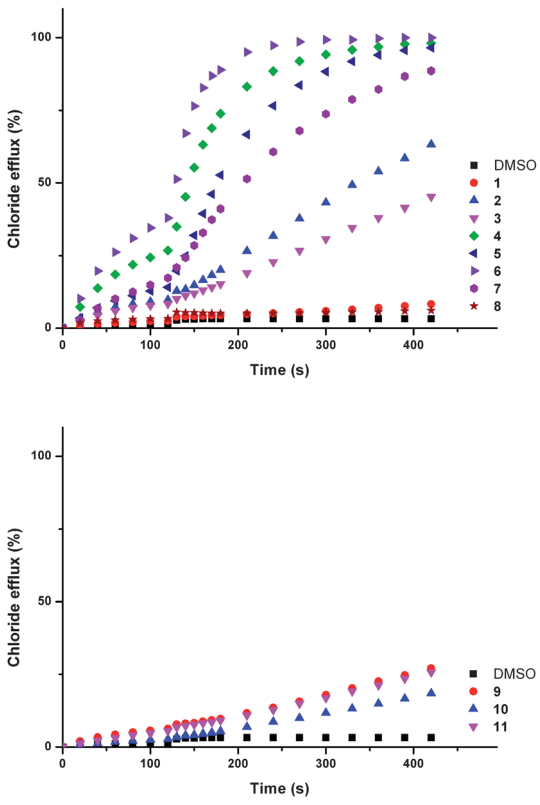


**Fig. 3** Chloride efflux promoted by a DMSO solution of compounds **1 12** (2 mol % carrier to lipid) from unilamellar POPC vesicles loaded with 451 mM NaCl buffered to pH 7.2 with 20 mM sodium phosphate salts. The vesicles were dispersed in 150 mM $Na_2SO_4$ buffered to pH 7.2 with 20 mM sodium phosphate salts. At $t = 120$ s a solution of sodium bicarbonate was added such that the external concentration of bicarbonate was 40 mM. At the end of the experiment, detergent was added to lyse the vesicles and calibrate the ISE to 100% chloride efflux. Each point represents an average of three trials. DMSO was used as a control. See Fig. S57 and S58† for versions of this figure with error bars.

Consequently, chloride efflux observed in the first two minutes of the assay (before the bicarbonate 'pulse') is not expected to be the result of an anion antiport mechanism. Upon addition of the 'bicarbonate pulse' a chloride/bicarbonate antiport mechanism becomes possible. A marked increase in transport activity was observed for compounds **2–7** at this point (Fig. 3).

Low levels of chloride efflux were observed for some of the compounds in the two minutes before the bicarbonate pulse in the aforementioned assay. To investigate this effect further, the experiment was repeated without the bicarbonate 'pulse'. Significant chloride efflux was observed for some of the compounds (see ESI, Fig. S59†).

Evidence in support of transmembrane sulfate transport has been observed previously for fluorinated tripodal ureas and thioureas.[44] To test if the chloride efflux observed in the aforementioned assay was linked to the transport of sulfate, unilamellar POPC vesicles were prepared containing 100 mM NaCl and 2 mM lucigenin buffered to pH 7.2 with 20 mM phosphate buffer. These vesicles were suspended in 100 mM NaCl solution buffered to pH 7.2 with 20 mM phosphate salts. A solution of sodium sulfate was added such that the external concentration of sulfate was 40 mM, and after one minute compounds **2–7** were added as solutions in methanol (2 mol% carrier to lipid). No evidence of sulfate transport was observed using this assay (see ESI†).

Compound **6** facilitated the highest chloride efflux in the sulfate 'blank' assay and was used to explore the possibility of HCl co-transport using a pH gradient assay.[45] Vesicles containing 451 mM sodium chloride buffered to pH 4.0 with 20 mM citric acid buffer were suspended in a solution of 150 mM sodium sulfate buffered to pH 7.2 with 20 mM sodium phosphate salts. Fig. 4 shows that the rate of chloride transport facilitated by compound **6** under gradient conditions is greater than in the absence of a pH gradient, implying that this molecule can facilitate HCl symport in addition to anion–anion antiport.

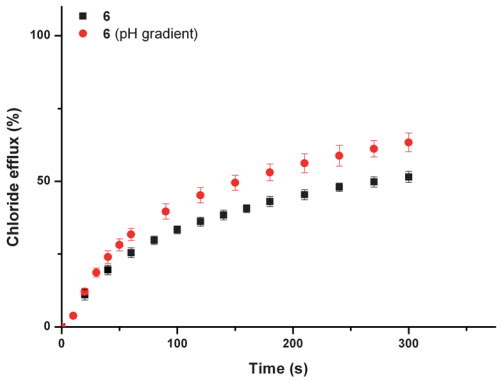


**Fig. 4** Chloride efflux promoted by a DMSO solution of compound **6** (2 mol% carrier to lipid) from unilamellar POPC vesicles loaded with either 451 mM NaCl buffered to pH 7.2 with 20 mM sodium phosphate salts or 451 mM NaCl buffered to pH 4.0 with 20 mM sodium citrate salts. The vesicles were dispersed in 150 mM $Na_2SO_4$ buffered to pH 7.2 with 20 mM sodium phosphate salts. At the end of the experiment, detergent was added to lyse the vesicles and calibrate the ISE to 100% chloride efflux. Each point represents an average of three trials. DMSO was used as a control.

Proton transport was confirmed using POPC vesicles loaded with NaCl (488 mM) and 1 mM 8-hydroxy-1,3,6-pyrenetrisulfonate (HPTS), a pH sensitive fluorescent dye.[46] These vesicles were suspended in a solution of $Na_2SO_4$ (150 mM) and the HPTS fluorescence measured upon addition of a DMSO solution of compound **6**. An increase in intravesicular pH was observed, corresponding to deacidification of the vesicles *via* either $H^+/Cl^-$ co-transport or an equivalent $Cl^-/OH^-$ antiport pathway (see ESI†).

Three modes of operation are known for synthetic transmembrane ion transporters; a mobile carrier mechanism, channel formation, or a relay mechanism.[47] We probed the transport mechanism of these systems using an ion selective electrode assay with POPC vesicles containing cholesterol (7 : 3 molar ratio). The vesicles were prepared containing sodium chloride (488 mM with 5 mM phosphate buffer at pH 7.2) and suspended in a solution of sodium nitrate (488 mM with 5 mM phosphate buffer at pH 7.2). By comparing the chloride efflux observed in this assay with that observed in the absence of cholesterol we can deduce if these molecules are mobile carriers. Cholesterol decreases membrane fluidity and thus transport that relies on a diffusion mechanism (*i.e.* mobile carrier), is expected to be slower in the presence of cholesterol.[48] Compounds **2–7** all showed reduced chloride efflux in the cholesterol containing vesicles (see ESI†).

Further evidence for a carrier mechanism was obtained from U-tube experiments.[15,44] A membrane is modelled by two aqueous phases separated by a nitrobenzene organic phase. The source phase was loaded with sodium chloride (488 mM buffered to pH 7.2 with 5 mM sodium phosphate salts) and the receiving phase was loaded with sodium nitrate (488 mM buffered to pH 7.2 with 5 mM sodium phosphate salts). The carrier (1 mM) was dissolved in the nitrobenzene phase and chloride transport into the receiving phase was monitored using an ion selective electrode. The separation of the two aqueous phases rules out the possibility of channel formation.[49] For solubility reasons only compounds **2**, **4**, **5** and **7** could be tested in this way. All yielded a higher concentration of chloride in the receiving phase than in the control (see ESI†). These results are further evidence that the compounds operate *via* a mobile carrier mechanism.

To quantify the transport activity of compounds **1–11** Hill analyses[50] for the chloride/nitrate and chloride/bicarbonate antiport assays were performed (see ESI†). Hill analysis enables determination of an $EC_{50,270s}$ value; the concentration of carrier (mol% with respect to lipid) required to afford 50% chloride efflux 270 s after addition of the carrier (or after the bicarbonate 'pulse'), enabling us to compare the transport activity of the compounds. These values are summarised in Table 2, together with the Hill coefficients (which provide supporting evidence for a mobile carrier mechanism), the calculated values for polar surface area (PSA) and total surface area (TSA) and log *P*.[51] The PSA and TSA parameters were estimated as described in the ESI† from molecular dynamic (MD) simulations carried out with compounds **1–11** in water solution.

In general, we observed that incorporation of electron withdrawing functionalities into the bisurea scaffold affords

**Table 2** Overview of transport assays, lipophilicity, PSA and TSA (average ± SD) of compounds **1** **11**

| | clogP[a] | PSA[b] (Å$^2$) | TSA[c] (Å$^2$) | $EC_{50,270s}$[d] ($Cl^-/NO_3^-$) | $n$[e] ($Cl^-/NO_3^-$) | $EC_{50,270s}$[d] ($Cl^-/HCO_3^-$) | $n$[e] ($Cl^-/HCO_3^-$) |
|---|---|---|---|---|---|---|---|
| **1** | 4.97 | 89.9 ± 7.1 | 482.7 ± 18.0 | na | na | na | na |
| **2**[f] | 5.80 | 155.5 ± 6.0 | 484.6 ± 17.9 | 0.14 | 0.9 | 1.40 | 0.7 |
| **3**[f] | 6.33 | 198.9 ± 6.7 | 530.0 ± 17.9 | 0.39 | 0.7 | >5 | 0.9 |
| **4**[f] | 4.72 | 203.6 ± 8.4 | 564.3 ± 23.2 | 0.011 | 0.7 | 0.073 | 1.0 |
| **5**[f] | 7.01 | 271.8 ± 11.9 | 601.8 ± 28.4 | 0.018 | 1.2 | 0.15 | 0.9 |
| **6**[f] | 4.58 | 286.0 ± 12.4 | 565.0 ± 27.1 | 0.0048 | 0.9 | 0.038 | 1.1 |
| **7**[f] | 4.58 | 263.4 ± 27.6 | 544.6 ± 40.4 | 0.084 | 1.0 | 0.21 | 0.8 |
| **8** | 4.58 | 203.0 ± 21.7 | 520.1 ± 21.8 | na | na | na | na |
| **9** | 3.20 | 114.1 ± 1.3 | 392.9 ± 2.9 | 1.76 | 1.8 | na | na |
| **10** | 4.35 | 150.2 ± 1.5 | 415.1 ± 3.0 | 1.80 | 2.1 | na | na |
| **11** | 3.13 | 157.5 ± 1.5 | 396.4 ± 2.9 | 1.05 | 1.5 | na | na |

[a] clogP calculated using Fieldview version 2.0.2 for Macintosh (Wildman Crippen model). [b] Polar surface area (PSA). [c] Total surface area (TSA). Both PSA and TSA values were calculated with MD simulations of 10 ns length (see ESI for details†). [d] $EC_{50,270s}$ defined as the concentration (mol% carrier to lipid) needed to obtain 50% chloride efflux after 270 s. [e] Hill coefficient. [f] Some of the transport activity observed may be the consequence of $H^+/Cl^-$ co transport.

**Table 3** Hammett substituent constants, $\sigma$, for moieties found in compounds **1** **11** (ref. 46)

| Compound | Substituent | $\sigma_{meta}$ | $\sigma_{para}$ |
|---|---|---|---|
| **1** | H | 0.00 | 0.00 |
| **2** | F | 0.34 | 0.06 |
| **3** | Cl | 0.37 | 0.23 |
| **4** | CN | | 0.66 |
| **5** | $CF_3$ | | 0.54 |
| **6** | $NO_2$ | | 0.78 |
| **7** | $NO_2$ | 0.71 | |
| **8** | $NO_2$ | | |
| **9** | CN | | 0.66 |
| **10** | $CF_3$ | | 0.54 |
| **11** | $NO_2$ | | 0.78 |

compounds capable of facilitating the transmembrane transport of anions. Parent compound **1** shows poor transport activity. Halogenation of the phenyl core in the 4- and 5-positions improved transporter activity, but to a less dramatic extent than the addition of electron withdrawing functionalities to the 4-position of the peripheral phenyl groups. In these instances transporter activity was observed to increase with increasing electron withdrawing strength of the substituents (represented by the Hammett constants shown in Table 3); H < F ~ Cl < $CF_3$ < CN < $NO_2$. This trend is consequently reflected in the binding constants, with transport inactive receptor **1** exhibiting relatively low binding constants with chloride and bicarbonate (43 $M^{-1}$ and 1270 $M^{-1}$ respectively), in comparison to the most active transporter **6**, (78 $M^{-1}$ and 3770 $M^{-1}$ respectively), reflecting the strong electron withdrawing effect of the nitro functionality. Indeed, *para*-nitro functionalised compound **6** displays very high transport activity, facilitating chloride efflux at receptor : lipid ratios as low as 1 : 1 000 000 (Fig. 5). To the best of our knowledge we believe that this is the lowest loading level of transporter observed that can facilitate transport to date.

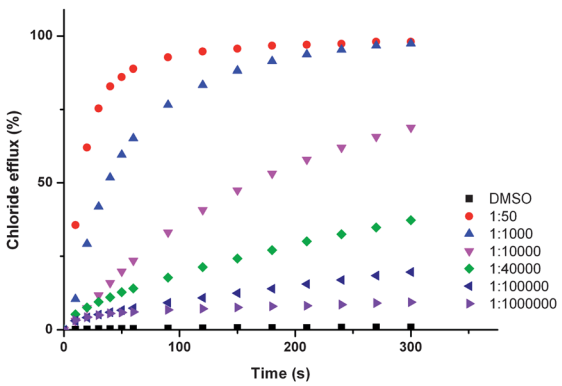


**Fig. 5** Chloride efflux promoted by a DMSO solution of compounds **6** at various loadings from unilamellar POPC vesicles loaded with 488 mM NaCl buffered to pH 7.2 with 5 mM sodium phosphate salts. The vesicles were dispersed in 488 mM $NaNO_3$ buffered to pH 7.2 with 5 mM sodium phosphate salts. At the end of the experiment detergent was added to lyse the vesicles and calibrate the ISE to 100% chloride efflux. Each point represents an average of three trials. DMSO was used as a control.

We have also examined the effect of varying substituent position on the peripheral phenyl rings (compounds **6**, **7**, and **8**). The nitro functionality is most electron withdrawing in the *ortho*- and *para*-positions.[52] *para*-Nitro functionalised compound **6** shows greater transporter activity than *meta*-nitro functionalised compound **7**. The *ortho*-nitro functionalised compound **8** displays poor transport activity, likely a consequence of the involvement of the nitro group in intramolecular hydrogen bonding and also sterically hindering the binding site.[17b] This is reflected in the stability constants for compound **8** with chloride and bicarbonate (<10 $M^{-1}$ and 826 $M^{-1}$ respectively) which are significantly lower than those observed for compounds **6** and **7**.

The transport activity of the monourea analogues of the three most active bisurea compounds (**4**, **5** and **6**) were tested using vesicles containing sodium chloride (488 mM with 5 mM phosphate buffer at pH 7.2) and suspended in a solution of sodium nitrate (488 mM with 5 mM phosphate buffer at pH 7.2). Compounds **9**, **10** and **11** were tested at loadings of 2 mol% (with respect to lipid), and the results compared to the efflux measured upon addition of compounds **4**, **5** and **6** at loadings of 1 mol% (with respect to lipid). This ensured that the concentration of *urea*

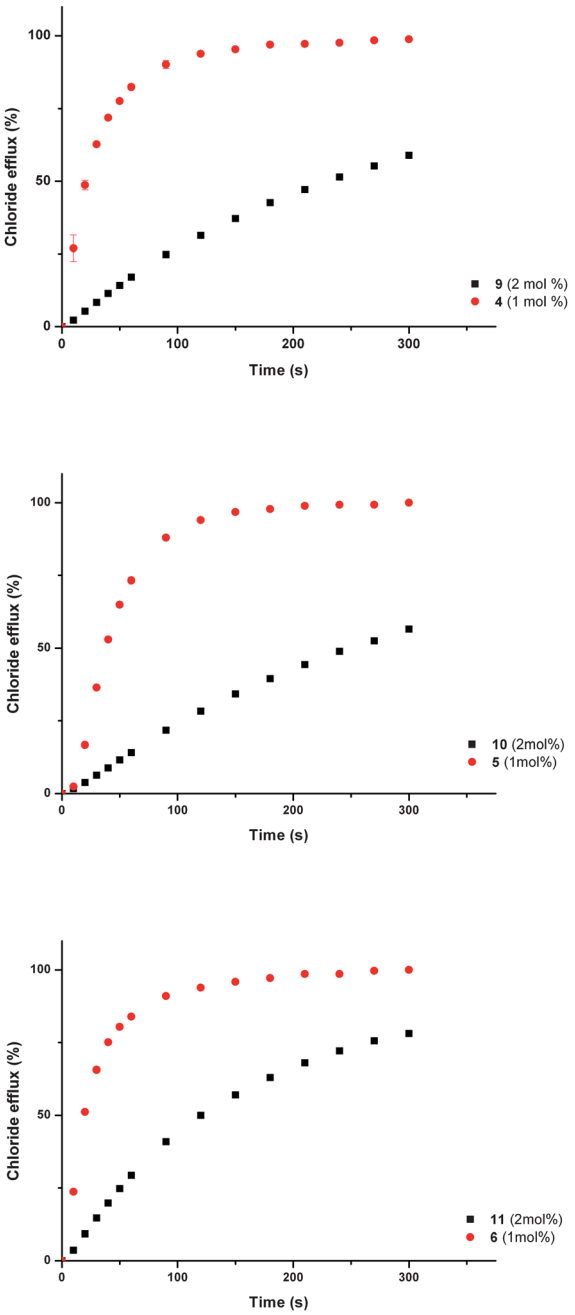


**Fig. 6** Chloride efflux promoted by a DMSO solution of monourea compounds **9** **11** (2 mol% carrier to lipid) and their analogous bisureas **4** **6** (1 mol% carrier to lipid) from unilamellar POPC vesicles loaded with 488 mM NaCl buffered to pH 7.2 with 5 mM sodium phosphate salts. The vesicles were dispersed in 488 mM $NaNO_3$ buffered to pH 7.2 with 5 mM sodium phosphate salts. At the end of the experiment detergent was added to lyse the vesicles and calibrate the ISE to 100% chloride efflux. Each point represents an average of three trials.

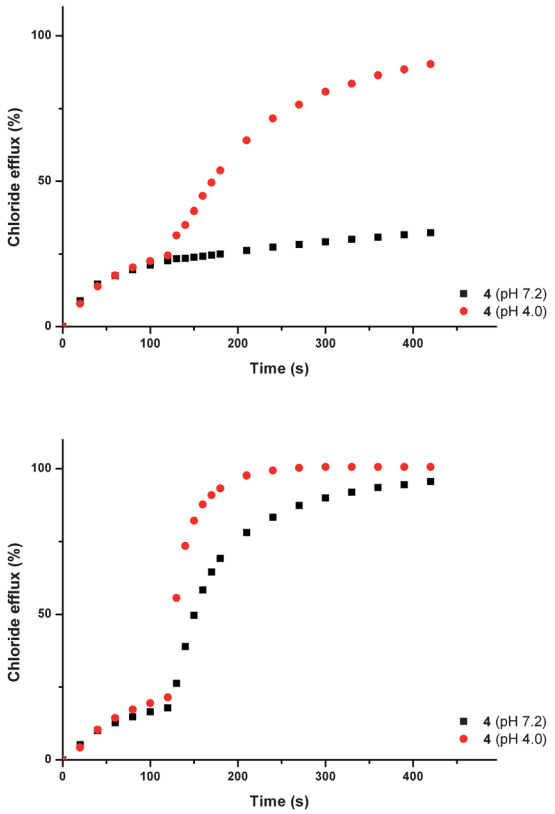


**Fig. 7** Chloride efflux promoted by a DMSO solution of compound **4** (2 mol% carrier to lipid) from unilamellar POPC vesicles loaded with either; (i) 451 mM NaCl buffered to pH 7.2 with 20 mM sodium phosphate salts and dispersed in 150 mM $Na_2SO_4$ buffered to pH 7.2 with 20 mM sodium phosphate salts, or (ii) 451 mM NaCl buffered to pH 4.0 with 20 mM sodium citrate salts and dispersed in 150 mM $Na_2SO_4$ buffered to pH 4.0 with 20 mM sodium citrate salts. At $t = 120$ s a solution of either sodium fumarate (top) or sodium maleate (bottom) was added such that the external concentration of carboxylate was 40 mM. At the end of the experiment, detergent was added to lyse the vesicles and calibrate the ISE to 100% chloride efflux. Each point represents an average of three trials. DMSO was used as a control.

*groups* was the same. The results (Fig. 6) show that the bisurea compounds are more active than their monourea analogues.

## Carboxylate transport

Recently, interest has grown in the construction of molecules capable of discriminating between small isomeric dicarboxylates.[53] Several examples of bisurea compounds with structural similarity to compounds **1–8**, have been shown to selectively bind carboxylates.[54] Owing to this similarity, we postulated that out most active transporters (**4**, **5** and **6**) might be able to facilitate the transmembrane transport of carboxylate anions. The transmembrane transport of carboxylates is biologically important; failure of glutamate transporters is linked neurodegenerative disorders including Alzheimer's and Huntingdon's disease,[55] whilst disruption of oxalate transport can result in renal disorders.[56]

We decided to focus on the transmembrane transport of fumarate and its stereoisomer, maleate. Fumarate has biological importance as a key intermediate in the citric acid cycle.[57] Carboxylate transport was examined using vesicles containing sodium chloride buffered to pH 7.2, suspended in a solution of sodium sulphate buffered at pH 7.2. Compounds **4**, **5** and **6** were added as solutions in DMSO (2 mol% with respect to lipid). After two minutes a sodium maleate or sodium fumarate 'pulse' was added such that the external concentration of the carboxylate was 40 mM. At pH 7.2 significant additional

chloride efflux was observed on addition of a sodium maleate 'pulse' with all three compounds, whilst no significant enhancement in chloride efflux was seen with the sodium fumarate 'pulse'. The experiment was repeated at pH 4.0, whereupon an enhancement in chloride efflux was observed upon addition of both maleate and fumarate pulses (Fig. 7 shows compound **4** as a representative example).

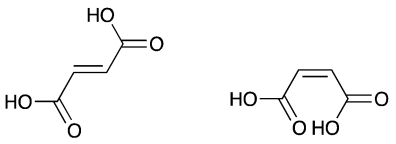


fumaric acid maleic acid

We have already shown that pre-pulse chloride efflux is the consequence of HCl symport and not sulfate transport or NaCl symport. We can rationalise the pH dependant nature of the transport by considering the p$K_a$ values for maleate (p$K_a$1 = 1.92, p$K_a$2 = 6.23) and fumarate (p$K_a$1 = 3.02, p$K_a$2 = 4.38).[52] Thus, at pH 7.2 a higher proportion of maleate exists as the monoanion, whilst fumarate will predominantly exist as the dianion. Dianions are more hydrophilic than their monoanionic counterparts and will consequently be more difficult to transport.[43] Hence, at pH 7.2 we observe an increase in chloride transport upon addition of maleate, but little enhancement upon addition of a fumarate. At pH 4.0 the monoionic forms of both maleate and fumarate will predominate, and an increase in chloride efflux was observed upon addition of both maleate and fumarate, corresponding to chloride/carboxylate exchange.

In summary, we have observed that *ortho*-phenylenediamine-based bisureas functionalised with electron withdrawing substituents are potent ion transporters, facilitating chloride/nitrate and chloride/bicarbonate antiport. In some instances we have observed carboxylate/chloride antiport and HCl symport. We have demonstrated that these compounds operate *via* a mobile carrier mechanism and that sulphate transport and metal/chloride symport processes are not facilitated.

## Cell based assays

The potent anion transport activity of some members of the series prompted examination of the *in vitro* cytotoxicity towards a range of cancerous cell lines. A single point MTT cell viability assay was performed with compounds **1**–**8** (10 μM) on a selection of cancer cell lines of diverse origin (human small-cell lung carcinoma GLC4, human alveolar adenocarcinoma A549, human colon adenocarcinoma SW480, human melanoma A375 and human oral adenosquamos carcinoma CAL27). Cell viability was assessed 48 hours after exposure to each of the compounds. Fig. 8 shows that compounds **2**, **5** and **8** display

**Table 4** $IC_{50}$ values (μM) of cytotoxic compounds **2**, **5** and **8** on GLC4, A549 and SW480 cancerous cell lines

| | GLC4 | A549 | SW480 |
|---|---|---|---|
| **2** | 8.0 ± 1.1 | 10.8 ± 0.7 | 10.6 ± 0.7 |
| **5** | 5.2 ± 0.1 | 6.0 ± 0.3 | 11.1 ± 2.0 |
| **8** | 5.0 ± 1.2 | 9.2 ± 2.2 | 3.3 ± 1.2 |

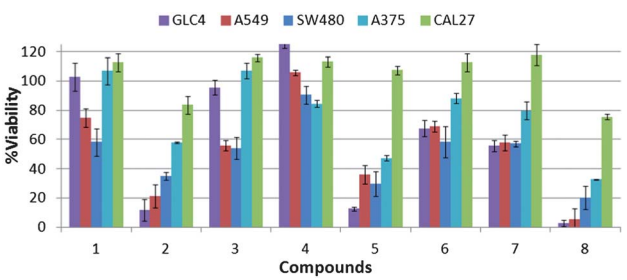


**Fig. 8** Cell viability after 48 h of compound treatment measured by MTT assay. Single point screening of compounds **1** **8** (10 μM) on a range of cancer cell lines, from left to right, GLC4, A549, SW480, A375 and CAL27.

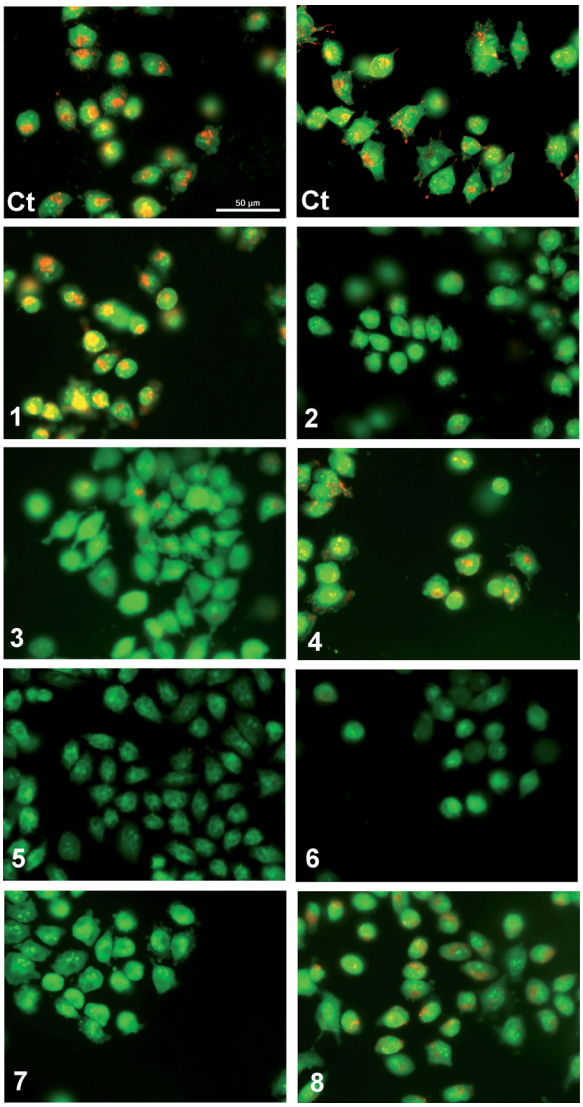


**Fig. 9** Acridine Orange staining of melanoma A375 cells after 1 hour exposure to compounds **1** **8** (50 μM): (Ct) control (untreated cells). Cells with cytoplasmic granular orange fluorescence (Ct, **1**, **4** and **8**); cells with a significant reduction in cytoplasmic orange fluorescence (**2** and **3**); cells with complete disappearance of cytoplasmic orange fluorescence (**5**, **6** and **7**).

significant cytotoxicity towards the GLC4, A549, SW480 and A375 cell lines. In comparison compounds **3**, **6** and **7** are less toxic, whilst compounds **1** and **4** are the least toxic in the series (Fig. 8).

Dose–response curve experiments were performed and $IC_{50}$ values (Inhibitory Concentration of 50% of cell population) were calculated for the most cytotoxic compounds (fluorinated compounds **2** and **5**, and nitro functionalised compound **8**) in the most sensitive cancerous cell lines (Table 4). These results corroborate the potency of these cytotoxic receptors, showing $IC_{50}$ values around 10 μM in GLC4 cells.

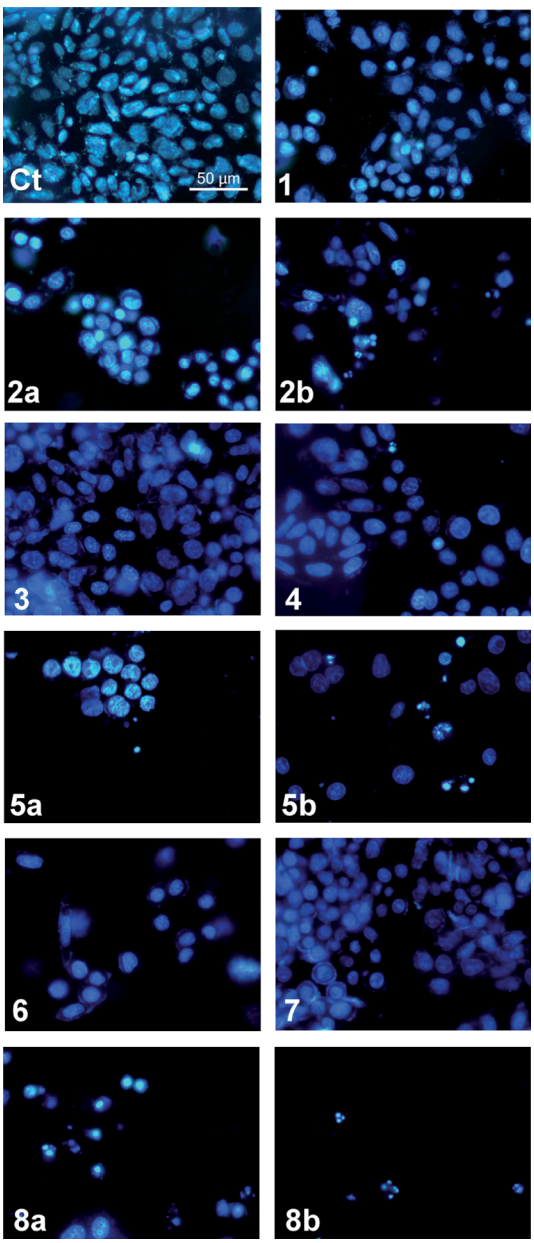


**Fig. 10** Hoechst 33342 staining of A375 cells after 48 hours exposure to compounds **1** **8** (10 μM or 10 μM (a) and 50 μM (b)): (Ct) control (untreated cells). Cells with typical nuclear morphology (Ct, 1, 3, 4 and 7), cells with nuclear condensation and apoptotic bodies (2a, 2b, 5a, 5b, 6, 8a, 8b).

We have previously reported that fluorination is an effective strategy for the production of compounds that can function as cytotoxic agents in cancerous cell lines.[15,44] In contrast, the nitrophenyl group is a known toxicophore.[58] The disruption of intracellular pH ($pH_i$) has been suggested as a strategy for cancer treatment.[59] Modulation of $pH_i$ is essential for control of the cell cycle (amongst other cellular processes) and is regulated by several mechanisms, including $Na^+/H^+$ co-transport, $Cl^-/HCO_3^-$ antiport, $Na^+/HCO_3^-$ symport and $H^+$ uniport.[60] To determine if the observed cytotoxicity was caused by sustained changes in $pH_i$ compounds **1–8** were studied in A375 melanoma cells stained with acridine orange (AO) (Fig. 9). Upon protonation this cell-permeable dye displays an orange fluorescence and accumulates within acidic intracellular compartments. Green fluorescence is observed under the more basic conditions of the cystol.[61] Cells in basal conditions were stained with AO and showed typical granular orange fluorescence, corresponding to cellular acidic compartments such as lysosomes (Fig. 9 Ct). A complete loss of orange fluorescence was observed on exposure to compounds **5**, **6** and **7** and a significant reduction in orange fluorescence was observed with compounds **2** and **3**. This corresponds to an increase in the pH of the intracellular organelles, achieved through acidification of the cytoplasm. Granular orange fluorescence was retained with compounds **1**, **4** and **8**, indicating that exposure to these compounds did not facilitate changes in $pH_i$. This finding, combined with the inactivity of compound **8** in the vesicle based ion transport assays, suggests that the cytotoxicity in this instance is the result of a mechanism other than transmembrane ion transport.[58]

Cancer cell death can be induced by sustained changes in $pH_i$.[62] Molecules capable of facilitating HCl symport and $Cl^-/HCO_3^-$ antiport have been shown to induce apoptosis by facilitating ion transport processes that lower $pH_i$.[15,44,63] All of the compounds that facilitated a reduction in $pH_i$ function as $Cl^-/NO_3^-$ and $Cl^-/HCO_3^-$ antiport agents in vesicle based assays. In addition, the most active transporter (compound **6**) has been shown to facilitate HCl co-transport. The biological activity observed in the AO assay could therefore be the direct result of the transmembrane transport of HCl or bicarbonate, or the result of ion transport coupled to the uniport of chloride.[64]

Apoptosis is a form of programmed cell death that facilitates the removal of damaged cells without causing inflammation and can be induced by sustained changes in $pH_i$. Nuclear condensation, fragmentation and the formation of apoptotic bodies are characteristic of this type of cell death.[65] The type of cell death induced by compounds **1–8** was examined using Hoechst 33342 staining in A375 cells. Hoechst 33342 is a fluorescent nuclear dye, permitting changes in nuclear morphology to be monitored. In Fig. 10 untreated A375 cells have typical rounded nuclei (Ct). Following treatment with the compounds (10 μM for 48 hours), the most cytotoxic compounds **2**, **5** and **8** showed nuclear condensation (2a, 5a, 8a), and at 50 μM the formation of apoptotic bodies was observed, confirming that these compounds induce apoptotic cell death (2b, 5b and 8b).

In summary, compounds **2**, **3**, **5**, **6**, **7** and **8** have been shown to be toxic in a range of cancer cell lines. With the exception of

compound **8**, all of the cytotoxic compounds were found to facilitate $Cl^-/NO_3^-$ and $Cl^-/HCO_3^-$ antiport in vesicle based ion transport assays. In an AO assay compounds **2**, **3**, **5**, **6** and **7** were found to alter $pH_i$ in A375 cells and the formation of apoptotic bodies was clearly observed with the most cytotoxic compounds (**2**, **5** and **8**) using Hoechst 33342 staining in A375 cells. Compounds **2** and **5** facilitated apoptotic cell death in A375 cells, likely through sustained changes in $pH_i$ as a consequence of *in vitro* ion transport. In contrast, compound **8** induced apoptotic cell death but organelle deacidification was not observed in the AO assay. The cytotoxicity of this compound thus appears to be unrelated to its ion transport activity (compound **8** was found to be inactive in vesicle based ion transport assays) and may therefore be the result of an alternative mechanism.[58] Compound **5** was shown to reduce the viability of the cell lines to a greater extent than compound **6** whilst compound **6** is the most effective anion transporter of the two compounds. This could be due to differences between the model membrane used for the vesicle studies and the biological membranes present in the cells. We are continuing to study the effects of these compounds on cells.

### Molecular dynamics simulations on POPC bilayer model

The ability of **5** and **6** to permeate a POPC bilayer model, being the first step towards the anion transport, was also investigated by molecular dynamics (MD) simulations using the AMBER12 software.[66] These mobile carriers were selected taking into account that, among the *ortho*-phenylendimine-based bisureas, **5** with two *p*-$CF_3$ substituents is significantly the more lipophilic one, while **6** functionalized with two *p*-$NO_2$ withdrawing electron substituents is the most active $Cl^-/HCO_3^-$ anion exchanger.

These modelling studies were carried out with **5**·$Cl^-$, **6**·$Cl^-$ and **5**·$HCO_3^-$ complexes and using a bilayer system (square in the *xy* plane), composed of 128 POPC lipids and 6500 TIP3P water molecules,[67] as model of a POPC vesicle. The compounds **5** and **6** and bicarbonate anion were described with GAFF[68] and RESP atomic charges (see ESI for details†), while the LIPID11 force field parameters[69] were used for the lipid molecules. The chloride anion and sodium counterion with respective net charges of 1 and +1 were described with van der Waals parameters developed for the TIP3P water model.[70] The

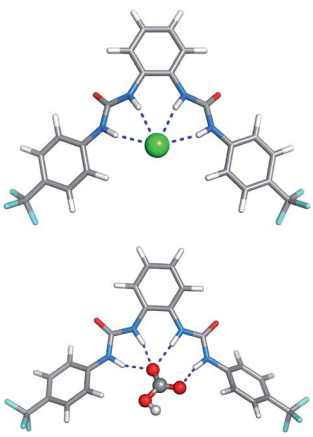

**Fig. 11** Molecular mechanics lowest energy structures of **5** Cl (top) and **5** $HCO_3$ (bottom) complexes, with N Cl distances ranging from 3.367 to 3.378 Å, and N O distances ranging from 2.748 to 2.873 Å.

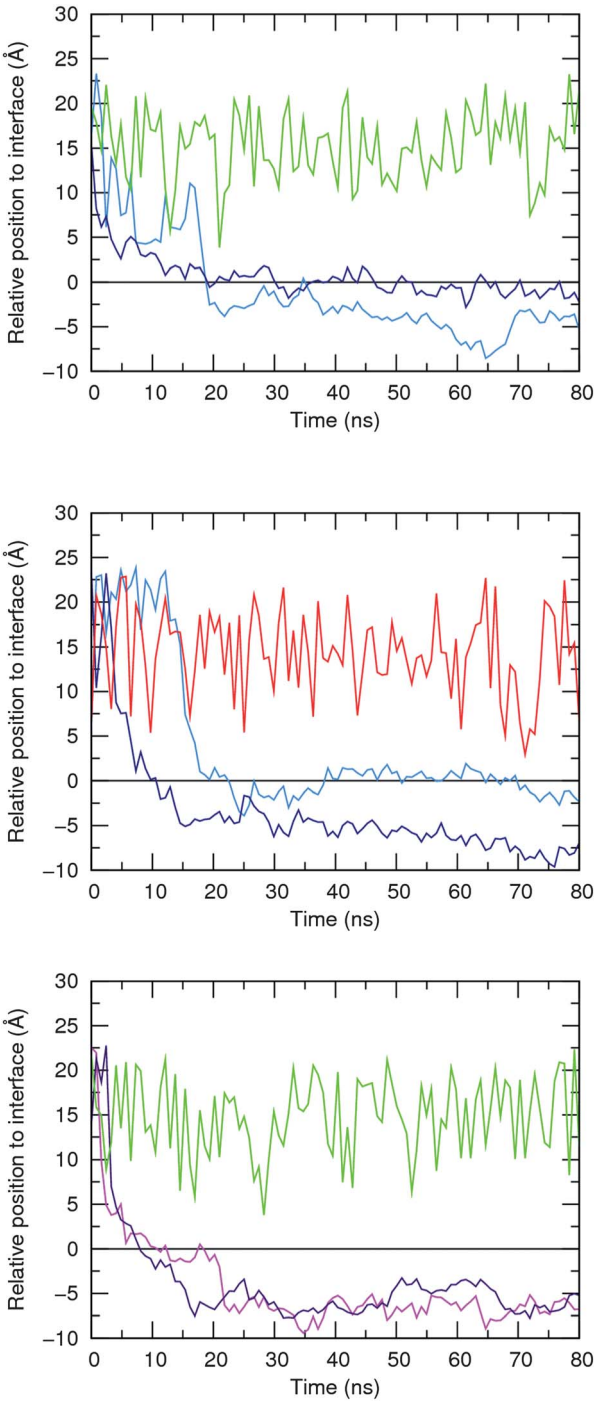


**Fig. 12** Relative positions of **5**, **6**, Cl and $HCO_3$ species defined by the distances between their centre of mass and the closest water lipid interface, which results from the average position of the corresponding phosphorus atoms in the *z* coordinate. Initial complexes per plot: **5** Cl top; **5** $HCO_3$ middle; and **6** Cl bottom. The following line colour scheme was used: light blue for R1 and dark blue for R2 of **5**; purple for R1 and magenta for R2 of **6**; green for Cl ; and red for $HCO_3$ . The water lipid interface is represented as a black line at $z = 0$ Å. Only the position of the anion along the replicate R1 is represented.

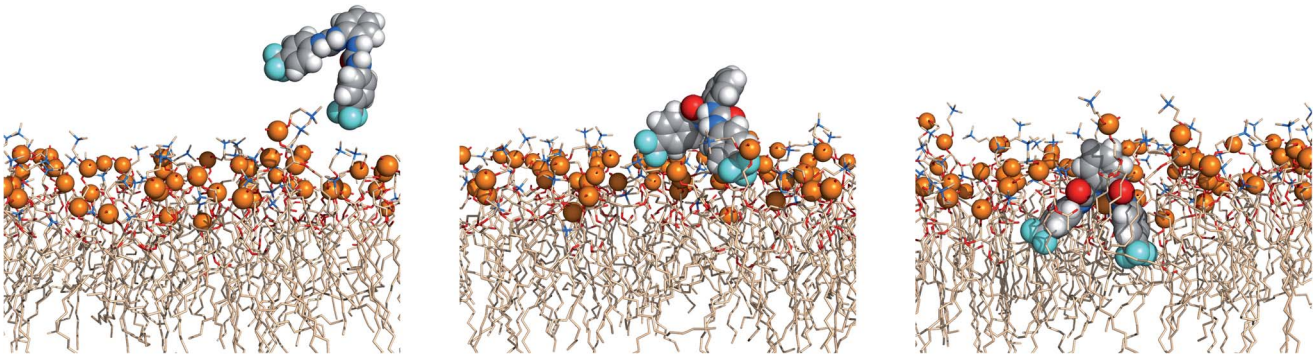

**Fig. 13** Passive diffusion of **5** Cl along the POPC bilayer showing the interaction of **5** with the phospholipid heads with three sequential snapshots taken from a representative MD replicate (R1). The receptor and phosphorus atoms are drawn in space filling fashion with hydrogen atoms in white, oxygen atoms in red, nitrogen atoms in light blue and carbon atoms in grey (receptor) or wheat (phospholipids) colour. The van der Waals radius of P was arbitrarily set to 1.2 Å. The water slabs and the second monolayer of phospholipids were omitted for clarity.



membrane simulations were performed under periodic boundary conditions in a NPT ensemble at 303 K with a surface tension of 17 dyn $cm^{-1}$ and an 8 Å cut-off for van der Waals and non-bonded electrostatic interactions following the protocol detailed in ESI.†

The starting binding arrangements of the anionic complexes were determined in gas phase by quenched molecular dynamics as stated in ESI.† In the lowest energy structures of the halide complexes, the two-bisurea binding sites adopt a *syn* configuration, establishing four N–H···$Cl^-$ hydrogen bonds. In the **5**·$HCO_3^-$ complex, three N–H binding sites form three N–H···O hydrogen bonds with an oxygen atom from the –$CO_2^-$ group while the remaining N–H binding site is involved in a N–H···O single hydrogen bond with the other oxygen atom from this group. These two binding scenarios are illustrated in Fig. 11 with the structures of **5**·$Cl^-$ and **5**·$HCO_3^-$ complexes, along with hydrogen bonds lengths.

Afterwards, **5**·$Cl^-$, **6**·$Cl^-$ and **5**·$HCO_3^-$ complexes were initially positioned in the water slab of a pre-equilibrated POPC bilayer at distances larger than 8 Å away from the water–lipid interface (see Fig. S95 in ESI†) and subject to a production run of 80 ns simulation length, preceded by a multi-stage equilibration process (see ESI†). Two independent replicates (R1 and R2) were performed for each system using different initial velocities and comparable sequences of events were observed as described below. The chloride and bicarbonate anions are promptly solvated by water molecules and released in the water phase before either **5** or **6** reach the water–lipid interface, which occurs within the first 20 ns of the production runs as depicted in Fig. 12 for all anion complexes. This first insight indicates that in the water phase, **5** displays equivalent binding behaviours towards both anions and henceforth the simulations carried out with **5**·$Cl^-$ and **5**·$HCO_3^-$ are analysed together. Afterwards, the free receptors interact with the membrane interface in a comparable fashion. Indeed, **5** is able to either permeate the membrane or to remain at the interface during almost of the subsequent simulation time, as also evident in Fig. 12 (top and middle plots). Surprisingly, the two replicates performed with **6**·$Cl^-$ reveal that this less lipophilic receptor (see Table 2) permeates the membrane more easily, which can be correlated with the population of N–H···O=P hydrogen bonds established between the amide binding sites and phosphate head groups, as discussed below.

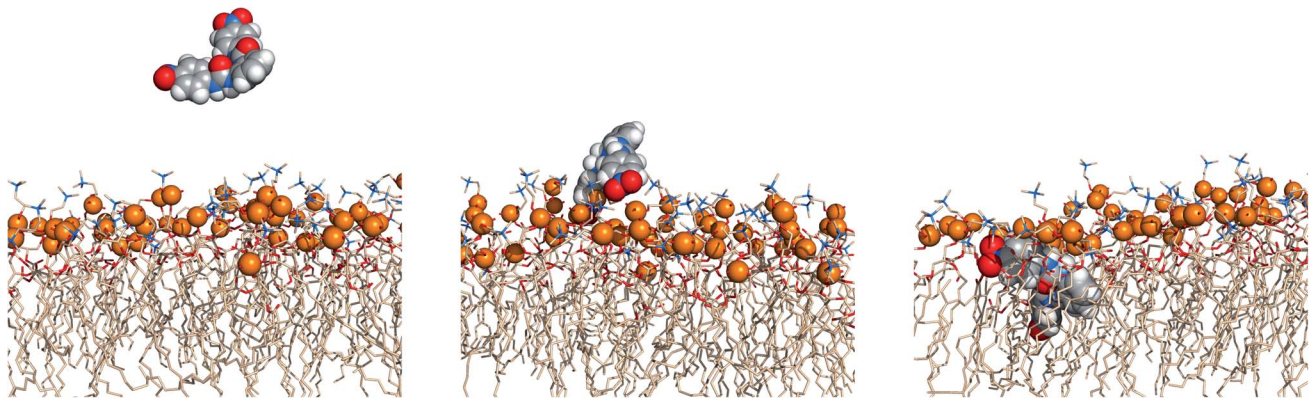

**Fig. 14** Passive diffusion of **6** Cl along POPC bilayer illustrated with three sequential snapshots of a representative MD replicate (R2). Remaining details as given in Fig. 13.

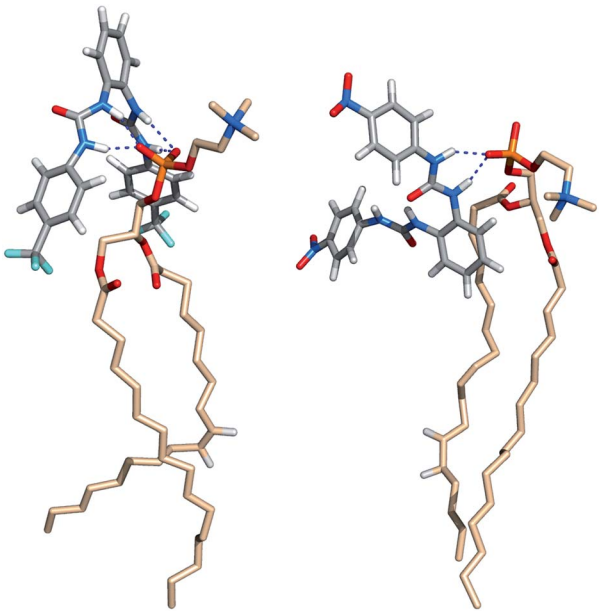

**Fig. 15** Insights into N H O=P hydrogen bonding interactions between phospholipids and transporters **5** (left) and **6** (right).

The events' sequences associated with the passive diffusion of **5** and **6** towards POPC, described above, are illustrated in Fig. 13 and 14 with three consecutive snapshots taken from the MD simulations of **5**·$Cl^-$ and **6**·$Cl^-$ complexes, respectively.

Fig. 13 and 14 show that the first interaction of **5** and **6** with membrane occurs through the *p*-$CF_3$ or *p*-$NO_2$ groups from an *ortho*-phenyldiamine substituent. Subsequently, regardless of the relative position of the receptors to the interface, both *p*-substituents of **5** are preferentially located between the lipids chains, pointing to the bilayer core, while the *ortho*-phenyldiamine head with the two *syn* urea binding units are closer to the water–lipid interface, thus able to form strong hydrogen bonding interactions with the phosphate head groups as shown in Fig. 15 (left). This is particularly evident in replicates R2 and R1 of complexes **5**·$Cl^-$ and **5**·$HCO_3^-$, respectively, where the receptor mainly remains at the water–lipid interface throughout the course of the MD simulation (see Fig. 12, top and middle plots, above and Fig. S96,† left and right top plots). In contrast, the slightly lighter receptor **6** (mol. wt 436.11 of **6** *vs.* 482.12 of **5**) permeates the phospholipid bilayer more deeply during the simulation time (see Fig. 12, bottom) with a non-specific spatial orientation consistent with the existence of sporadic N–H···O=P hydrogen bonds. These interactions generally occur *via* a single urea binding unit, as depicted in Fig. 15 (right), and are observed during both MD simulations replicates of **6**·$Cl^-$ (see Fig. S96,† bottom), in spite of this receptor higher propensity to establish hydrogen bonding interactions (see Table 3). In other words, these results seem to indicate that N–H binding sites of **6** are available to bind the anions and consequently to promote their transmembrane transport, in agreement with the chloride efflux experimental data.

**Table 5** Average structural parameters area per lipid (Å$^2$) and bilayer thickness (Å) of membrane systems, with the corresponding standard deviations[a]

| System | | Area | Thickness |
|---|---|---|---|
| *Pure membrane* | | | |
| Experimental[71] | | 64.30 | 39.10 |
| Simulated | | 64.38 ± 0.74 | 38.28 ± 0.37 |
| *Transporters in POPC* | | | |
| **5**·Cl | R1 | 62.16 ± 0.53 | 39.34 ± 0.24 |
| | R2 | 61.25 ± 0.49 | 39.80 ± 0.31 |
| **5**·$HCO_3$ | R1 | 62.67 ± 0.74 | 39.30 ± 0.44 |
| | R2 | 61.50 ± 0.77 | 39.97 ± 0.30 |
| **6**·Cl | R1 | 62.39 ± 0.40 | 39.14 ± 0.23 |
| | R2 | 61.79 ± 0.91 | 39.67 ± 0.61 |

[a] The sampling time for the pure membrane was 40 ns, while the remaining systems were analysed during the final 10 ns of the MD simulation time.

In order to ascertain the impact of **5** and **6** on the structural properties of the POPC bilayer, the aforementioned simulations were preceded by a simulation of the free membrane under the same computational conditions. The following structural membrane parameters, area per lipid, bilayer thickness, electronic density profile and order parameters were evaluated and compared with the corresponding experimental data and with those found for the last 10 ns of MD replicates of **5**·$Cl^-$, **6**·$Cl^-$ and **5**·$HCO_3^-$ complexes. The first two parameters' values are listed in Table 5, whereas the corresponding electronic density profiles and order parameters are plotted in Fig. S100 to S105.† As would be expected, the average values of the area per lipid (64.38 Å$^2$) and bilayer thickness (38.28 Å) calculated for the free membrane are similar to those recently obtained by neutron scattering (64.30 Å$^2$ and 39.10 Å),[71] and as reported when a POPC bilayer with 128 lipids is simulated using the aforementioned simulation conditions.[69] The interaction of **5** and **6** with the membrane produces a slight decrease in the area per lipid (<4.8%) and, consequently, a slight increase in the bilayer thickness (<2.2%), indicating that the influence of both receptors on these two structural parameters is small. The order parameters for saturated (*sn*-1) and unsaturated (*sn*-2) POPC lipid chains of the free membrane (see Fig. S99†) follow the ones previously found with LIPID11.[69] Similar profiles were obtained for the membrane simulations carried out with **5** and **6** (see Fig. S103 to S105†), suggesting that the order parameters are unaffected by the presence of the receptors. In fact, the single exception was found for the *sn*-2 tails of POPC in replicate R2 of **5**·$Cl^-$ in which the receptor is preferentially located near of the water–lipid interface. Furthermore, the electronic density profiles for all simulated systems show that the bilayer structure is preserved without apparent interdigitation between the phospholipid tails as shown in Fig. S100 to S102, and further discussed in ESI.† In addition, the electronic density profiles for the receptors are consistent with their relative position to the water–lipid interface throughout the simulation time, as represented in Fig. 12.

The energy profiles associated with $Cl^-$ and $HCO_3^-$ facilitated transport across a phospholipid bilayer by *ortho*-phenylenediamine-based bisureas (namely **4**, **5** and **6**), as well as the theoretical investigation of $Cl^-/HCO_3^-$ exchange mechanisms in more complex membrane systems (models of vesicles) and

 

more computationally demanding, are currently in progress. However, the studies reported here have unequivocally shown that two of the most promising receptors are able to permeate the membrane, having a low impact in its structure, being capable of mediating anion transport as mobile carriers.

## Conclusions

We have demonstrated that the *ortho*-phenylenebisurea motif is a new scaffold for the construction of transmembrane ion transporters that function by an anion antiport and in some cases a HCl co-transport mechanism. Addition of electron withdrawing groups to either the central core or the peripheral phenyl groups yielded potent anion transporters for the transmembrane transport of chloride, nitrate and bicarbonate with transport observed at receptor: lipid concentration ratios as low as 1 : 1 000 000. Compounds **2**, **3**, **5**, **6** and **7** were found to be cytotoxic in a range of cancer cell lines. AO assays confirmed that these compounds can facilitate a reduction in $pH_i$ and the two most cytotoxic compounds (**2** and **5**) were found to induce apoptosis in A375 cells. We have also demonstrated that our most active transporters (**4**, **5** and **6**) can facilitate the transmembrane transport of carboxylate species. We are continuing to study the transport of biologically relevant carboxylates. The results of these studies will be reported in due course. The MD results have demonstrated, at the atomic level, the ability of **5** and **6** to permeate the membrane while having a reduced influence on its properties.

## Acknowledgements

PAG thanks the EPSRC for a PhD studentship (SJM) and for access to the crystallographic facilities at the University of Southampton.[72] CJEH thanks the EPSRC for a Doctoral Prize. This work was supported by a research grant from the Spanish government and the European Union (FIS-PI10/00338). The modelling studies were supported by the FEDER, through the Operational Program Competitiveness Factors – COMPETE and National Funds through FCT (Fundação para a Ciência e a Tecnologia) under project PTDC/QUI-QUI/101022/2008. PJC thanks FCT for the postdoctoral grant SFRH/BPD/27082/2006.

## Notes and references

1 J. I. Korenbrot, *Annu. Rev. Physiol.*, 1977, **39**, 19–49.
2 F. M. Ashcroft, *Ion Channels and Disease*, Academic Press, San Diego, 2000.
3 E. Cordat and J. R. Casey, *Biochem. J.*, 2009, **417**, 423–439.
4 (*a*) P. M. Quinton, *Lancet*, 2008, **372**, 415–417; (*b*) A. S. Garcia, N. Yang and P. M. Quinton, *J. Clin. Invest.*, 2009, **119**, 2613–2622.
5 (*a*) N. Altan, Y. Chen, M. Schindler and S. M. Simon, *J. Exp. Med.*, 1998, **187**, 1583–1598; (*b*) Y. Chen, M. Schindler and S. M. Simon, *J. Biol. Chem.*, 1999, **274**, 18364–18373; (*c*) S. Matsuyama, J. Llopis, Q. L. Deveraux, R. Y. Tsien and J. C. Reed, *Nat. Cell Biol.*, 2000, **2**, 318–325.
6 For an excellent overview of the chemistry of the prodigiosins related to their structural, anion transport and anti-cancer properties see: (*a*) J. T. Davis, in *Topics in Heterocyclic Chemistry*, ed. P. A. Gale and W. Dehaen, Springer-Verlag, Berlin Heidelberg, 2010, vol. 24, pp. 145–176. See also: (*b*) T. Sato, H. Konno, Y. Tanaka, T. Kataoka, K. Nagai, H. H. Wasserman and S. Ohkuma, *J. Biol. Chem.*, 1998, **273**, 21455–21462; (*c*) J. L. Sessler, L. R. Eller, W.-S. Cho, S. Nicolaou, A. Aguilar, J. T. Lee, V. M. Lynch and D. J. Magda, *Angew. Chem., Int. Ed.*, 2005, **44**, 5989–5992; (*d*) A. Fürstner, *Angew. Chem., Int. Ed.*, 2003, **42**, 3582–3603; (*e*) J. L. Seganish and J. T. Davis, *Chem. Commun.*, 2005, 5781–5783; (*f*) H. Konno, H. Matsuya, M. Okamoto, T. Sato, Y. Tanaka, K. Yokoyama, T. Kataoka, K. Nagai, H. H. Wasserman and S. Ohkuma, *J. Biochem.*, 1998, **124**, 547–556; (*g*) J. T. Davis, P. A. Gale, O. A. Okunola, P. Prados, J. C. Iglesias-Sánchez, T. Torroba and R. Quesada, *Nat. Chem.*, 2009, **1**, 138–144; (*h*) M. Nguyen, R. C. Marcellus, A. Roulston, M. Watson, L. Serfass, S. R. M. Madiraju, D. Goulet, J. Viallet, L. Bélec, X. Billot, S. Acoca, E. Purisima, A. Wiegmans, L. Cluse, R. W. Johnstone, P. Beauparlant and G. C. Shore, *Proc. Natl. Acad. Sci. U. S. A.*, 2007, **104**, 19512–19517.
7 (*a*) B. A. McNally, A. V. Koulov, B. D. Smith, J.-B. Joos and A. P. Davis, *Chem. Commun.*, 2005, 1087–1089; (*b*) A. P. Davis and J.-B. Joos, *Coord. Chem. Rev.*, 2003, **240**, 143–156; (*c*) A. P. Davis, *Coord. Chem. Rev.*, 2006, **250**, 2939–2951; (*d*) B. A. McNally, A. V. Koulov, T. N. Lambert, B. D. Smith, J.-B. Joos, A. L. Sisson, J. P. Clare, V. Sgarlata, L. W. Judd, G. Magro and A. P. Davis, *Chem.–Eur. J.*, 2008, **14**, 9599–9606.
8 (*a*) C. C. Tong, R. Quesada, J. L. Sessler and P. A. Gale, *Chem. Commun.*, 2008, 6321–6323; (*b*) P. A. Gale, C. C. Tong, C. J. E. Haynes, O. Adeosun, D. E. Gross, E. Karnas, E. M. Sedenberg, R. Quesada and J. L. Sessler, *J. Am. Chem. Soc.*, 2010, **132**, 3240–3241; (*c*) M. G. Fisher, P. A. Gale, J. R. Hiscock, M. B. Hursthouse, M. E. Light, F. P. Schmidtchen and C. C. Tong, *Chem. Commun.*, 2009, 3017–3019.
9 S. K. Berezin and J. T. Davis, *J. Am. Chem. Soc.*, 2009, **131**, 2458–2459; S. Bahmanjah, N. Zhang and J. T. Davis, *Chem. Commun.*, 2012, **48**, 4432–4434.
10 P. V. Santacroce, J. T. Davis, M. E. Light, P. A. Gale, J. C. Iglesias-Sánchez, P. Prados and R. Quesada, *J. Am. Chem. Soc.*, 2007, **129**, 1886–1887; N. Busschaert, I. L. Kirby, S. Young, S. J. Coles, P. N. Horton, M. E. Light and P. A. Gale, *Angew. Chem., Int. Ed.*, 2012, **51**, 4426–4430.
11 N. Busschaert, P. A. Gale, C. J. E. Haynes, M. E. Light, S. J. Moore, C. C. Tong, J. T. Davis and W. A. Harrell, Jr, *Chem. Commun.*, 2010, **46**, 6252–6254.
12 (*a*) H. Grasemann, F. Stehling, H. Brunar, R. Widmann, T. W. Laliberte, L. Molina, G. Döring and F. Ratjen, *Chest*, 2007, **131**, 1461–1466; (*b*) I. Izzo, S. Licen, N. Maulucci, G. Autore, S. Marzocco, P. Tecilla and F. De Riccardis, *Chem. Commun.*, 2008, 2986–2988; (*c*) X. Li, B. Shen, X.-Q. Yao and D. Yang, *J. Am. Chem. Soc.*, 2009, **131**, 13676–13680.

13 (*a*) M. P. Gleeson, *J. Med. Chem.*, 2008, **51**, 817–834; (*b*) E. H. Kerns and L. Di, *Drug-like Properties: Concepts, Structure Design and Methods*, Academic Press, Amsterdam, 2008.
14 (*a*) C. A. Lipinski, F. Lombardo, B. W. Dominy and P. J. Feeney, *Adv. Drug Delivery Rev.*, 1997, **23**, 3–25; (*b*) C. A. Lipinski, *J. Pharmacol. Toxicol. Methods*, 2000, **44**, 235–249.
15 S. J. Moore, M. Wenzel, M. E. Light, R. Morley, S. J. Bradberry, P. Gómez-Iglesias, V. Soto-Cerrato, R. Pérez-Tomás and P. A. Gale, *Chem. Sci.*, 2012, **3**, 2501–2508.
16 C. J. E. Haynes, S. J. Moore, J. R. Hiscock, I. Marques, P. J. Costa, V. Félix and P. A. Gale, *Chem. Sci.*, 2012, **3**, 1436–1444.
17 (*a*) S. J. Brooks, P. A. Gale and M. E. Light, *Chem. Commun.*, 2005, 4696–4698; (*b*) S. J. Brooks, P. R. Edwards, P. A. Gale and M. E. Light, *New J. Chem.*, 2006, **30**, 65–70.
18 Y.-J. Kim, H. Kwak, S. J. Lee, J. S. Lee, H. J. Kwon, S. H. Nam, K. Lee and C. Kim, *Tetrahedron*, 2006, **62**, 9635–9640.
19 S. J. Brooks, P. A. Gale and M. E. Light, *Supramol. Chem.*, 2007, **19**, 9–15.
20 (*a*) C. Jia, B. Wu, S. Li, Z. Yang, Q. Zhao, J. Liang, Q.-S. Li and X.-J. Yang, *Chem. Commun.*, 2010, **46**, 5376–5378; (*b*) C. Jia, B. Wu, S. Li, X. Huang and X.-J. Yang, *Org. Lett.*, 2010, **12**, 5612–5615.
21 C. Jia, B. Wu, S. Li, X. Huang, Q. Zhao, Q.-S. Li and X.-J. Yang, *Angew. Chem., Int. Ed.*, 2011, **50**, 486–490.
22 (*a*) S. J. Brooks, P. A. Gale and M. E. Light, *Chem. Commun.*, 2006, 4344–4346; (*b*) S. J. Brooks, S. E. García-Garrido, M. E. Light, P. A. Cole and P. A. Gale, *Chem.–Eur. J.*, 2007, **13**, 3320–3329.
23 (*a*) H. Yang, Z.-G. Zhou, J. Xu, F.-Y. Li, T. Yi and C.-H. Huang, *Tetrahedron*, 2007, **63**, 6732–6736; (*b*) D. A. Jose, D. K. Kumar, B. Ganguly and A. Das, *Tetrahedron Lett.*, 2005, **46**, 5343–5346.
24 V. Amendola, M. Boiocchi, D. Esteban-Gómez, L. Fabbrizzi and E. Monzani, *Org. Biomol. Chem.*, 2005, **3**, 2632–2639.
25 M. O. Odago, D. M. Colabello and A. J. Lees, *Tetrahedron*, 2010, **66**, 7465–7471.
26 (*a*) S. J. Brooks, P. A. Gale and M. E. Light, *CrystEngComm*, 2005, **7**, 586–591; (*b*) S. Li, M. Wei, X. Huang, X.-J. Yang and B. Wu, *Chem. Commun.*, 2012, **48**, 3097–3099.
27 J. van Esch, F. Schoonbeek, M. de Loos, H. Kooijman, A. L. Spek, R. M. Kellogg and B. Feringa, *Chem.–Eur. J.*, 1999, **5**, 937–950.
28 (*a*) C. Bied, J. J. E. Moreau and M. W. C. Man, *Tetrahedron: Asymmetry*, 2001, **12**, 329–336; (*b*) E. G. Klauber, C. K. De, T. K. Shah and D. Seidel, *J. Am. Chem. Soc.*, 2010, **132**, 13624–13626.
29 (*a*) M. T. Bogert and L. E. Wise, *J. Am. Chem. Soc.*, 1912, **34**, 693–702; (*b*) L. Peyron and J. Peyron, *Bull. Soc. Chim.*, 1953, **9**, 846–852; (*c*) S. N. Gavade, R. S. Balaskar, M. S. Mane, P. N. Pabrekar, M. S. Shingare and D. V. Mane, *Chin. Chem. Lett.*, 2011, **22**, 675–678.
30 (*a*) J. Scheele, P. Timmerman and D. N. Reinhoudt, *Chem. Commun.*, 1998, 2613–2614; (*b*) Y. Ge, L. Miller, T. Ouimet and D. K. Smith, *J. Org. Chem.*, 2000, **65**, 8831–8838.
31 (*a*) P. Grammaticakis, *Bull. Soc. Chim.*, 1959, **10**, 1559–1570; (*b*) H. Iwamura, T. Fujita, S. Koyama, K. Koshimizu and Z. Kumazawa, *Phytochemistry*, 1980, **19**, 1309–1319.
32 (*a*) M. Miyahara, *Chem. Pharm. Bull.*, 1986, **34**, 1950–1960; (*b*) G. A. Artamkina, A. G. Sergeev and I. P. Beletskava, *Russ. J. Org. Chem.*, 2002, **38**, 538–545; (*c*) G. A. Artamkina, A. G. Sergeev and I. P. Beletskaya, *Tetrahedron Lett.*, 2001, **42**, 4381–4384; (*d*) B. J. Kotecki, D. P. Fernando, A. R. Haight and K. A. Lukin, *Org. Lett.*, 2009, **11**, 947–950.
33 (*a*) N. J. Andrews, C. J. E. Haynes, M. E. Light, S. J. Moore, C. C. Tong, J. T. Davis, W. A. Harrell Jr and P. A. Gale, *Chem. Sci.*, 2011, **2**, 256–260; (*b*) P. A. Gale, J. R. Hiscock, S. J. Moore, C. Caltagirone, M. B. Hursthouse and M. E. Light, *Chem.–Asian J.*, 2010, **5**, 555–561.
34 M. J. Hynes, *J. Chem. Soc., Dalton Trans.*, 1993, 311–312.
35 A. Barnard, S. J. Dickson, M. J. Paterson, A. M. Todd and J. W. Steed, *Org. Biomol. Chem.*, 2009, **7**, 1554–1561.
36 (*a*) M. Boiocchi, L. Del Boca, D. Esteban-Gómez, L. Fabbrizzi, M. Licchelli and E. Monzani, *Chem.–Eur. J.*, 2005, **11**, 3097–3104; (*b*) D. Esteban-Gómez, L. Fabbrizzi and M. Licchelli, *J. Org. Chem.*, 2005, **70**, 5717–5720; (*c*) V. Amendola, D. Esteban-Gómez, L. Fabbrizzi and M. Licchelli, *Acc. Chem. Res.*, 2006, **39**, 343–353; (*d*) M. Bonizzoni, L. Fabbrizzi, A. Taglietti and F. Tiengo, *Eur. J. Org. Chem.*, 2006, 3567–3574; (*e*) S. E. García-Garrido, C. Caltagirone, M. E. Light and P. A. Gale, *Chem. Commun.*, 2007, 1450–1452.
37 Y. Shao, B. Linton, A. D. Hamilton and S. G. Weber, *J. Electroanal. Chem.*, 1998, **441**, 33–37.
38 E. N. Kitova, A. El-Hawiet, P. D. Schnier and J. S. Klassen, *J. Am. Soc. Mass Spectrom.*, 2012, **23**, 431–441.
39 L. Jaquillard, F. Saab, F. Schoentgen and M. Cadene, *J. Am. Soc. Mass Spectrom.*, 2012, **23**, 908–922.
40 (*a*) B. D. Smith and T. N. Lambert, *Chem. Commun.*, 2003, 2261–2268; (*b*) A. V. Koulov, T. N. Lambert, R. Shukla, M. Jain, J. M. Boon, B. D. Smith, H. Li, D. N. Sheppard, J.-B. Joos, J. P. Clare and A. P. Davis, *Angew. Chem., Int. Ed.*, 2003, **42**, 4931–4933.
41 M. Yano, C. C. Tong, M. E. Light, F. P. Schmidtchen and P. A. Gale, *Org. Biomol. Chem.*, 2010, **8**, 4356–4363.
42 (*a*) W. W. Cleland, T. J. Andrews, S. Gutteridge, F. C. Hartman and G. H. Lorimer, *Chem. Rev.*, 1998, **98**, 549–561; (*b*) A.-V. Rousselle and D. Heymann, *Bone*, 2002, **30**, 533–540; (*c*) D. Bok, G. Galbraith, I. Lopez, M. Woodruff, S. Nusinowitz, H. BeltrandelRio, W. Huang, S. Zhao, R. Geske, C. Montgomery, I. van Sligtenhorst, C. Friddle, K. Platt, M. J. Sparks, A. Pushkin, N. Abuladze, A. Ishiyama, R. Dukkipati, W. Liu and I. Kurtz, *Nat. Genet.*, 2003, **34**, 313–319; (*d*) R. D. Vaughan-Jones, K. W. Spitzer and P. Swietach, *J. Mol. Cell. Cardiol.*, 2009, **46**, 318–331.
43 Y. Marcus, *J. Chem. Soc., Faraday Trans.*, 1991, **87**, 2995–2999.
44 N. Busschaert, M. Wenzel, M. E. Light, P. Iglesias-Hernández, R. Pérez-Tomás and P. A. Gale, *J. Am. Chem. Soc.*, 2011, **133**, 14136–14148.
45 P. A. Gale, J. Garric, M. E. Light, B. A. McNally and B. D. Smith, *Chem. Commun.*, 2007, 1736–1738.

46 N. R. Clement and J. M. Gould, *Biochemistry*, 1981, **20**, 1534–1538.
47 (*a*) A. P. Davis, D. N. Sheppard and B. D. Smith, *Chem. Soc. Rev.*, 2007, **36**, 348–357; (*b*) A. L. Sisson, M. R. Shah, S. Bhosale and S. Matile, *Chem. Soc. Rev.*, 2006, **35**, 1269–1286; (*c*) B. A. McNally, E. J. O'Neil, A. Nguyen and B. D. Smith, *J. Am. Chem. Soc.*, 2008, **130**, 17274–17275; (*d*) G. W. Gokel and N. Barkey, *New J. Chem.*, 2009, **33**, 947–963; (*e*) J. T. Davis, O. Okunola and R. Quesada, *Chem. Soc. Rev.*, 2010, **39**, 3843–3862; (*f*) P. A. Gale, *Acc. Chem. Res.*, 2011, **44**, 216–226.
48 C. Kirby, J. Clarke and G. Gregoriadis, *Biochem. J.*, 1980, **186**, 591–598.
49 O. Murillo, I. Suzuki, E. Abel, C. L. Murray, E. S. Meadows, T. Jin and G. W. Gokel, *J. Am. Chem. Soc.*, 1997, **119**, 5540–5549.
50 (*a*) A. V. Hill, *Biochem. J.*, 1913, **7**, 471–480; (*b*) S. Bhosale and S. Matile, *Chirality*, 2006, **18**, 849–856.
51 (*a*) P. Ertl, B. Rohde and P. Selzer, *J. Med. Chem.*, 2000, **43**, 3714–3737; (*b*) S. A. Wildman and G. M. Crippen, *J. Chem. Inf. Comput. Sci.*, 1999, **39**, 868–873; (*c*) *Fieldview version 2.0.2 for Macintosh*, Cresset, 2011.
52 (*a*) D. H. McDaniel and H. C. Brown, *J. Org. Chem.*, 1958, **23**, 420–427; (*b*) S. R. Crouch, D. A. Skoog, D. M. West and F. J. Holler, Analytical Chemistry, An Introduction, 7th edn, Brooks/Cole, Belmont CA, USA, 1999, Appendix 2, p. A-3.
53 (*a*) F. Sancenón, R. Martínez-Máñez, M. A. Miranda, M.-J. Seguí and J. Soto, *Angew. Chem., Int. Ed.*, 2003, **42**, 647–650; (*b*) A. M. Costero, M. Colera, P. Gaviña and S. Gil, *Chem. Commun.*, 2006, 761–763; (*c*) J. C. Kim, A. J. Lough, H. Park and Y. C. Kang, *Inorg. Chem. Commun.*, 2006, **9**, 514–517; (*d*) Y.-P. Yen and K.-W. Ho, *Tetrahedron Lett.*, 2006, **47**, 7357–7361; (*e*) Y.-P. Tseng, G.-M. Tu, C.-H. Lin, C.-T. Chang, C.-Y. Lin and Y.-P. Yen, *Org. Biomol. Chem.*, 2007, **5**, 3592–3598; (*f*) S. Goswami, N. K. Das, D. Sen, G. Hazra, J. H. Goh, Y. C. Sing and H.-K. Fun, *New J. Chem.*, 2011, **35**, 2811–2819.
54 (*a*) E. Fan, S. A. Van, S. Kincaid and A. D. Hamilton, *J. Am. Chem. Soc.*, 1993, **115**, 369–370; (*b*) T. R. Kelly and M. H. Kim, *J. Am. Chem. Soc.*, 1994, **116**, 7072–7080; (*c*) K.-S. Jeong, J. W. Park and Y. L. Cho, *Tetrahedron Lett.*, 1996, **37**, 2795–2798; (*d*) R. J. Fitzmaurice, G. M. Kyne, D. Douheret and J. D. Kilburn, *J. Chem. Soc., Perkin Trans. 1*, 2002, 841–864.
55 (*a*) E. Foran and D. Trotti, *Antioxid. Redox Signaling*, 2009, **11**, 1587–1602; (*b*) J.-H. Yi and A. S. Hazell, *Neurochem. Int.*, 2006, **48**, 394–403; (*c*) E. Masliah, L. Hansen, M. Alford, R. Deteresa and M. Mallory, *Ann. Neurol.*, 1996, **40**, 759–766; (*d*) S. Li, M. Mallory, M. Alford, S. Tanaka and E. Masliah, *J. Neuropathol. Exp. Neurol.*, 1997, **56**, 901–911; (*e*) P. F. Behrens, P. Franz, B. Woodman, K. S. Lindenberg and G. B. Landwehrmeyer, *Brain*, 2002, **125**, 1908–1922.
56 J. S. Clark, D. H. Vandrope, M. N. Chernova, J. F. Heneghan, A. K. Stewart and S. L. Alper, *J. Physiol.*, 2008, **586**, 1291–1306.
57 H. A. Krebs, *The Citric Acid Cycle*, Nobel Lecture, 1953.
58 (*a*) J. Kazius, R. McGuire and R. Bursi, *J. Med. Chem.*, 2005, **48**, 312–320; (*b*) Q. Li, M. Minami, T. Hanaoka and Y. Yamamura, *Toxicology*, 1999, **137**, 35–45; (*c*) K. Shinoda, K. Mitsumori, K. Yasuhara, C. Uneyama, H. Onodera, K. Takegawa, M. Takahashi and T. Umemura, *Arch. Toxicol.*, 1998, **72**, 296–302; (*d*) M. Sajan, G. Reddy and A. P. Kulkarni, *Int. J. Toxicol.*, 2000, **19**, 285–292; (*e*) Y. Ohkuma and S. Kawanishi, *Biochem. Biophys. Res. Commun.*, 1999, **257**, 555–560.
59 M. F. McCarty and J. Whitaker, *Alternative Med. Rev.*, 2010, **15**, 264–272.
60 I. H. Madshus, *Biochem. J.*, 1988, **250**, 1–8.
61 A. C. Allison and M. R. Young, *Lysosomes in Biology and Pathology*, North-Holland Publishing Co., Amsterdam, 1969, vol. 2.
62 M. Yamagate and I. F. Tannock, *Br. J. Cancer*, 1996, **73**, 1328–1334.
63 R. Pérez-Tomás, B. Montaner, E. Llagostera and V. Soto-Cerrato, *Biochem. Pharmacol.*, 2003, **66**, 1447–1452; P. I. Hernández, D. Moreno, A. A. Javier, T. Torroba, R. Pérez-Tomás and R. Quesada, *Chem. Commun.*, 2012, **48**, 1556–1558.
64 S. J. Moore, M. G. Fisher, M. Yano, C. C. Tong and P. A. Gale, *Dalton Trans.*, 2011, **40**, 12017–12020; S. J. Moore, M. G. Fisher, M. Yano, C. C. Tong and P. A. Gale, *Chem. Commun.*, 2011, **47**, 689–691.
65 A. De Milito, E. Lessi, M. Logozzi, F. Lozupone, M. Spada, M. L. Marino, C. Federici, M. Perdicchio, P. Matarrese, L. Lugini, A. Nilsson and S. Fais, *Cancer Res.*, 2007, **67**, 5408–5417.
66 D. A. Case, T. A. Darden, T. E. Cheatham, III, C. L. Simmerling, J. Wang, R. E. Duke, R. Luo, R. C. Walker, W. Zhang, K. M. Merz, B. Roberts, S. Hayik, A. Roitberg, G. Seabra, J. Swails, A. W. Götz, I. Kolossváry, K. F. Wong, F. Paesani, J. Vanicek, R. M. Wolf, J. Liu, X. Wu, S. R. Brozell, T. Steinbrecher, H. Gohlke, Q. Cai, X. Ye, J. Wang, M.-J. Hsieh, G. Cui, D. R. Roe, D. H. Mathews, M. G. Seetin, R. Salomon-Ferrer, C. Sagui, V. Babin, T. Luchko, S. Gusarov, A. Kovalenko, and P. A. Kollman, *AMBER 12*, University of California, San Francisco, 2012.
67 W. L. Jorgensen, J. Chandrasekhar, J. D. Madura, R. W. Impey and M. L. Klein, *J. Chem. Phys.*, 1983, **79**, 926–935.
68 (*a*) J. Wang, R. M. Wolf, J. W. Caldwell, P. A. Kollman and D. A. Case, *J. Comput. Chem.*, 2004, **25**, 1157–1174; (*b*) J. Wang, R. M. Wolf, J. W. Caldwell, P. A. Kollman and D. A. Case, *J. Comput. Chem.*, 2005, **26**, 114.
69 (*a*) Å. A. Skjevik, B. D. Madej, R. C. Walker and K. Teigen, *J. Phys. Chem. B*, 2012, DOI: 10.1021/jp3059992; (*b*) R. C. Walker and B. Madej, private communication, 2012.
70 I. S. Joung and T. E. Cheatham, *J. Phys. Chem. B*, 2008, **112**, 9020–9041.
71 N. Kučerka, M.-P. Nieh and J. Katsaras, *Biochim. Biophys. Acta, Biomembr.*, 2011, **1808**, 2761–2771.
72 S. J. Coles and P. A. Gale, *Chem. Sci.*, 2012, **3**, 683–689.